Supplement of Wu et al.

A Model for Urban Biogenic CO_2 Fluxes: Solar-Induced Fluorescence for Modeling Urban biospheric Fluxes ("SMUrF")

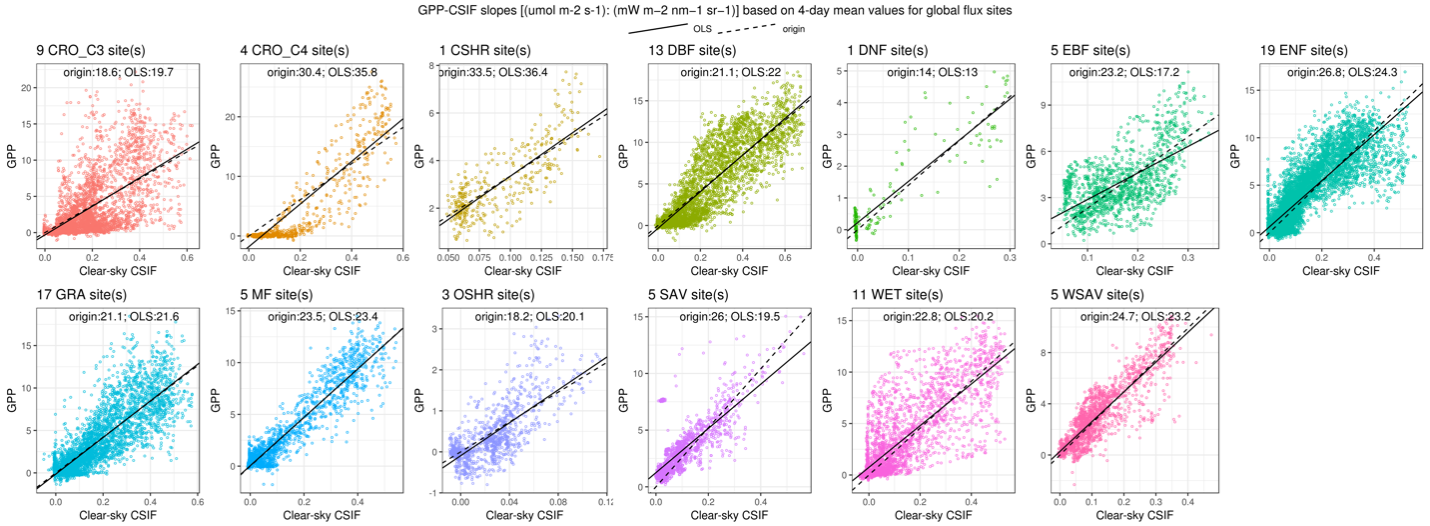

Figure S1. GPP-CSIF slopes [(umol m^{-2} s^{-1}): (mW m^{-2} nm^{-1} sr^{-1})] based on 4-day mean GPP and CSIF across 12 different natural biomes from 98 flux sites around the globe. Both linear fits across the origin (dashed lines) and fits using the Ordinary least squares (OLS) regressions have been plotted (solid lines) with slopes printed on the top of each panel.

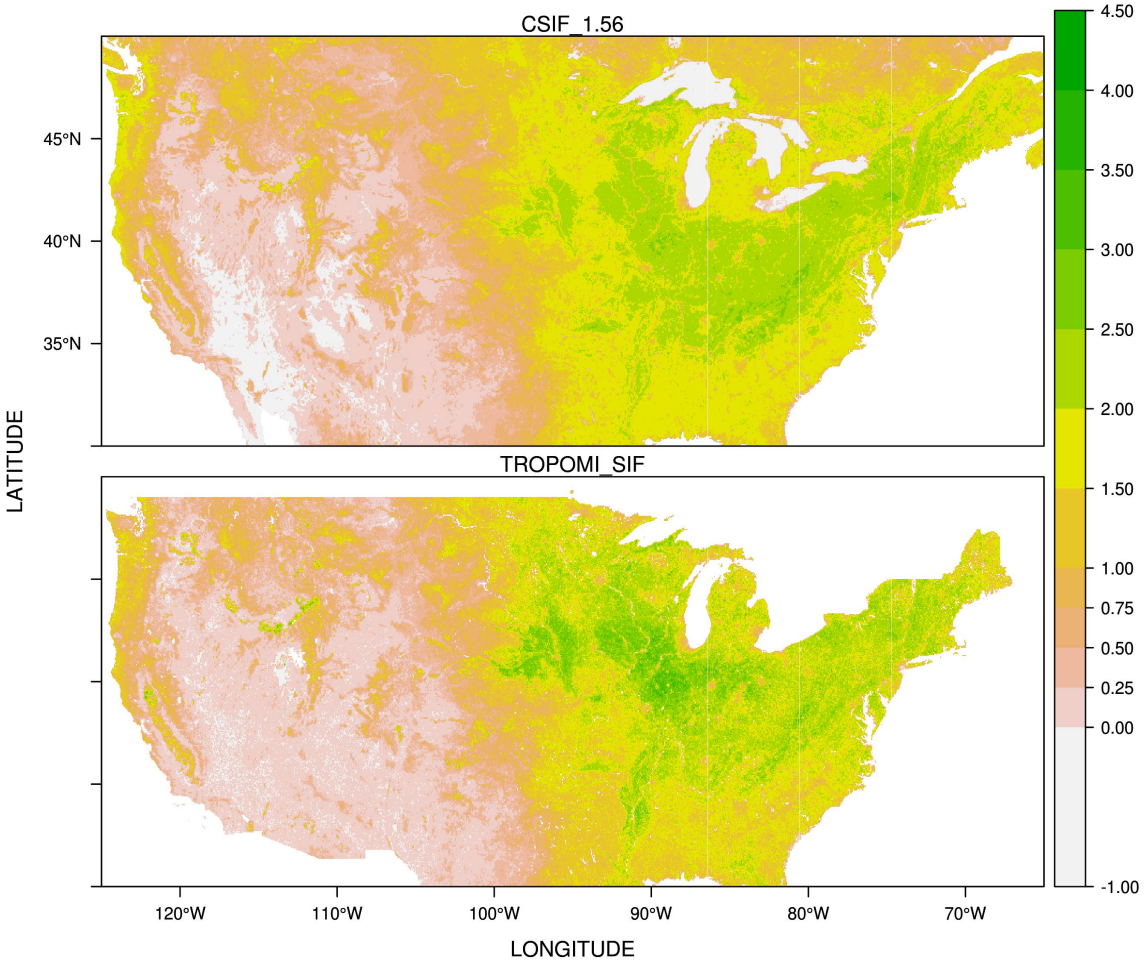

Figure S2. Comparison between instantaneous CSIF and TROPOMI SIF (mW m^{-2} nm^{-1} sr^{-1}, at the overpass time of ~1 pm vs. 1:30 pm), averaged over all days during JJA 2018 at a grid spacing of 0.05º. Downscaled TROPOMI SIF is initially available at 500 m horizontal grid spacing and then re-projected to CSIF grid and CSIF has been scaled up.

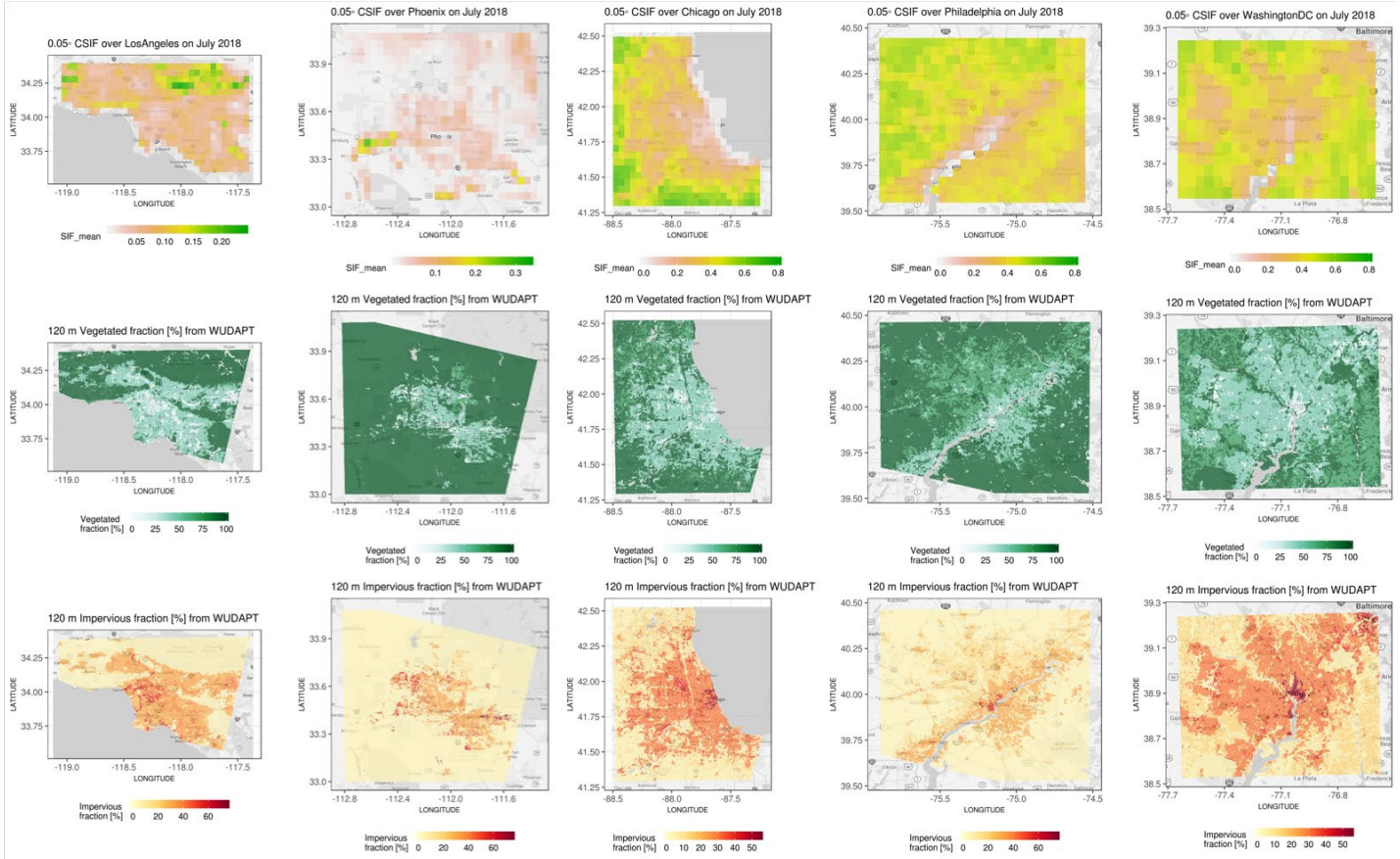

Figure S3. Mean 0.05° CSIF over July 2018 (1st row) and 120 m vegetated fractions and impervious fractions from WUDAPT (2nd and 3rd rows) for Los Angeles, Phoenix, Chicago, Philadelphia, and Washington DC.

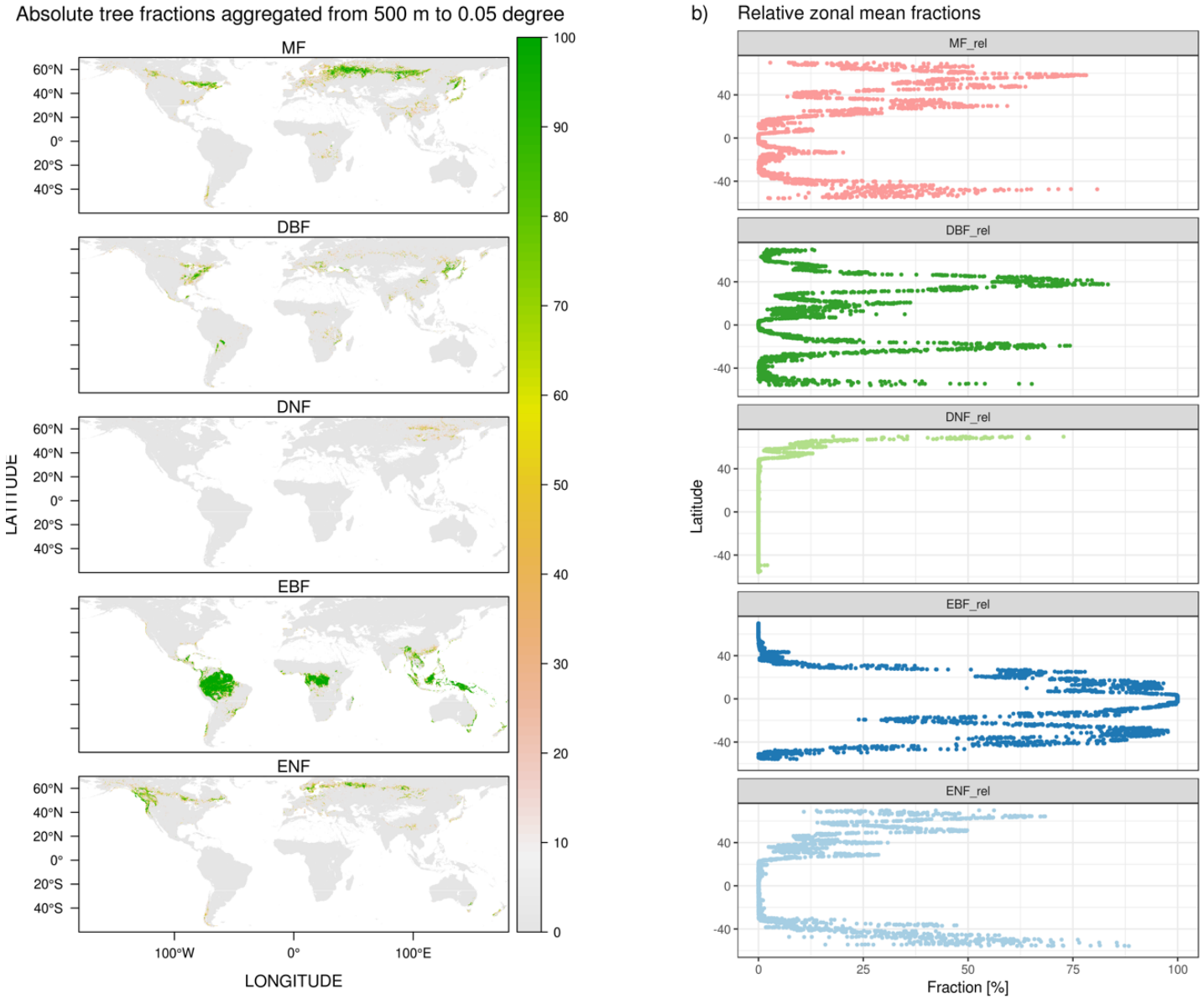

Figure S4. Fractions of mixed, deciduous broadleaf, deciduous needleleaf, evergreen broadleaf, and evergreen needleleaf forests aggregated at 0.05° from 500 m MCD12Q1 (**a**) and their relative fractions averaged over the longitude (zonal mean fractions in **b**). These fractions are used as a climatological latitude-dependence for approximating urban vegetation types and fractions.

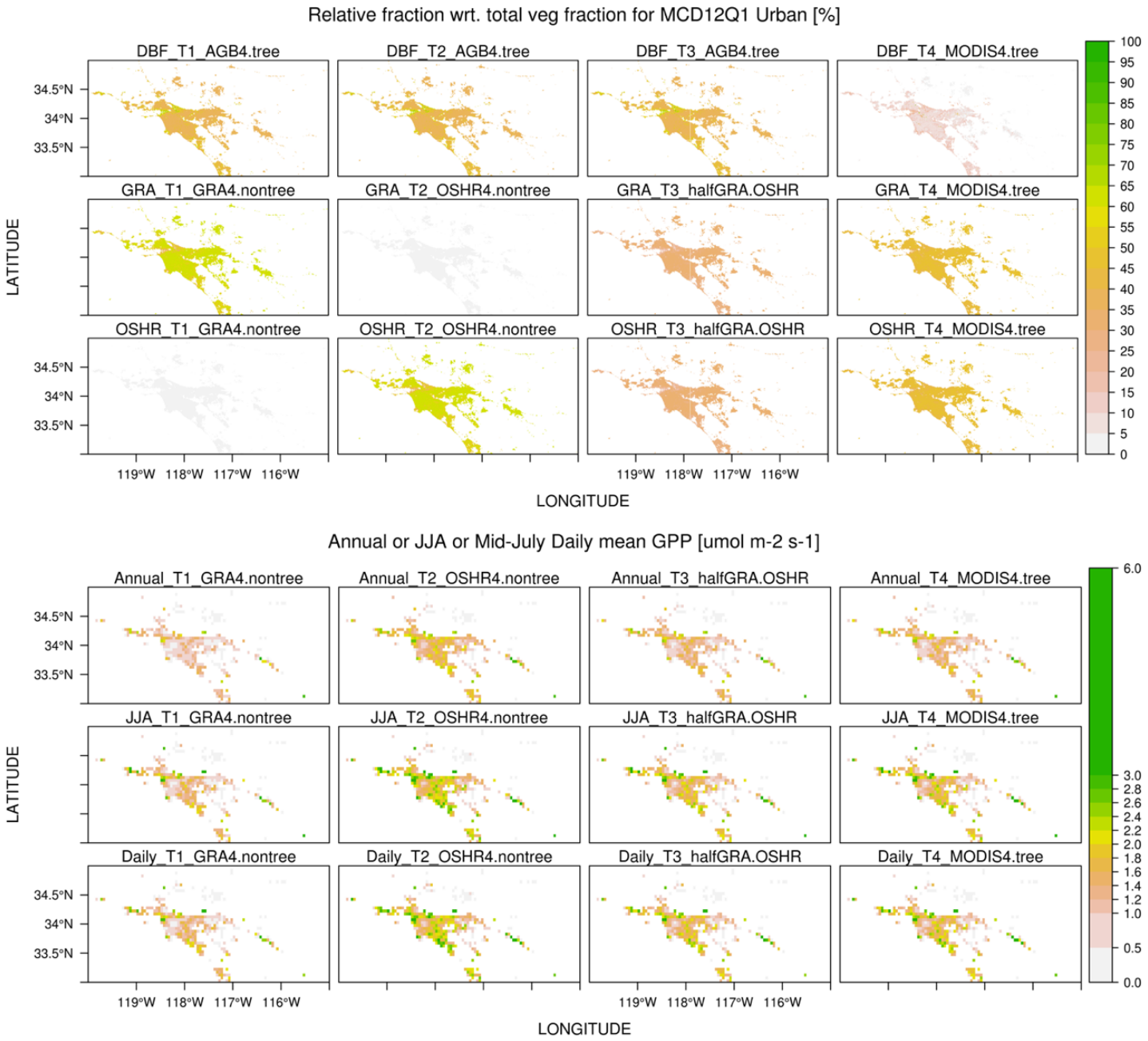

Figure S5. A sensitivity test of the impact of different assumptions for predicting vegetation fractions (upper panels) on final annual, summertime, and daily mean GPP fluxes (lower panels). Each column represents a separate test as follows:

1st column (T1): DBF fractions based on AGB-derived tree fractions, non-tree fractions as **GRA** (i.e., no OSHR);

2nd column (T2): DBF fractions based on AGB-derived tree fractions, non-tree fractions as **OSHR** (i.e., no GRA);

3rd column (T3): DBF fractions based on AGB-derived tree fractions, non-tree fractions as **half GRA & half OSHR**;

4th column (T4): DBF fractions based on MOD44B tree fractions, treat non-tree fractions as **half GRA & half OSHR**.

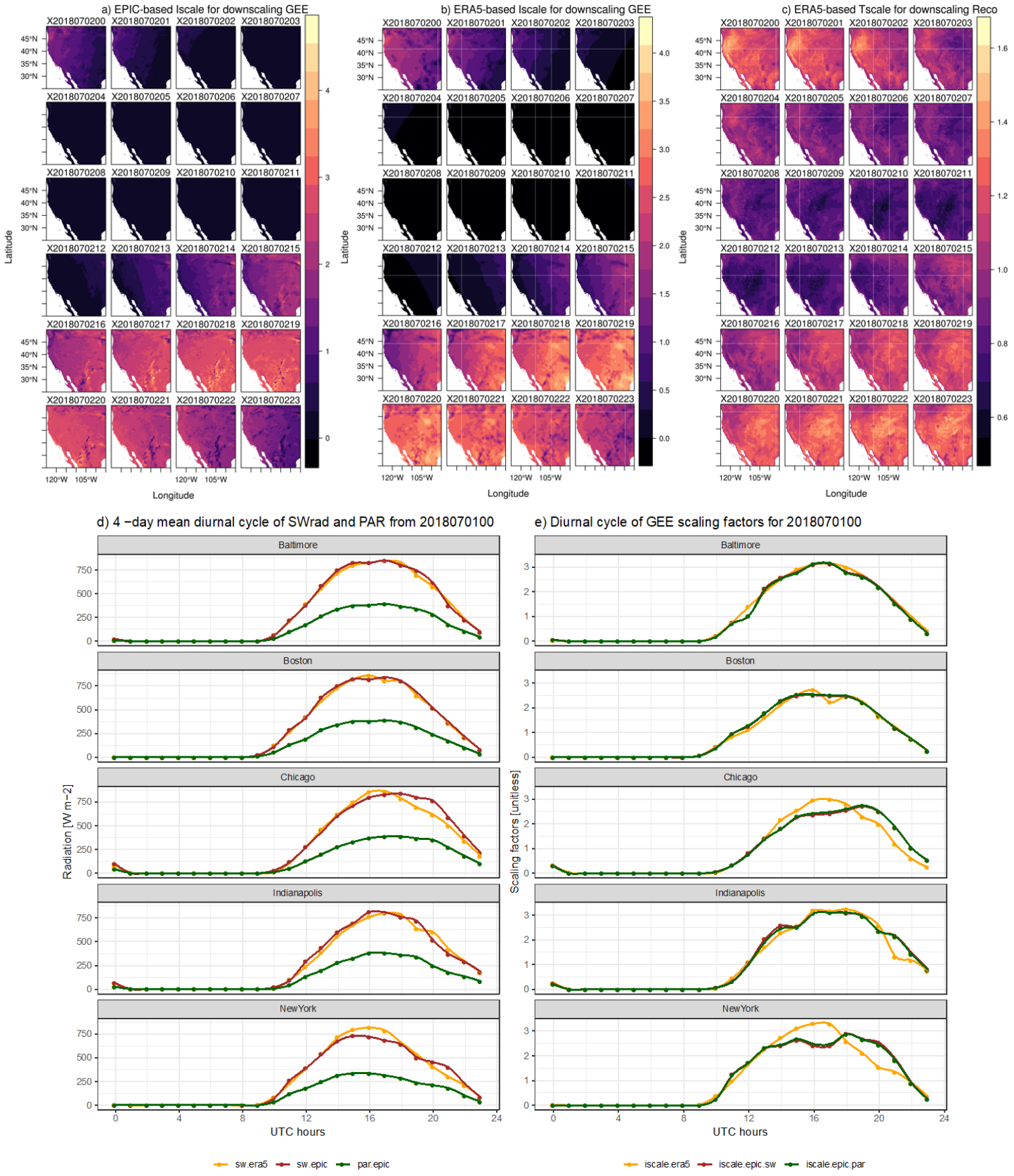

Figure S6. Examples of hourly scaling factors for GPP and R_{eco}. I_{scale} and T_{scale} are calculated based on SW radiation received at the surface with account of cloud coverage using EPIC (panel a) or ERA5 (panel b) and the ERA5-based air temperature dependent Q10 functions (c) for the western CONUS on 07/02/2018. UTC times are denoted above each panel (e.g., 1200 UTC = 0800 ET; 16UTC = 1200 ET, etc) **d-e)** 4-day mean SW_{rad} (orange or red lines) or PAR (dark green lines) from two models (d) as well as hourly I_{scale} calculated using those radiation products (e), interpolated to 5 eastern US cities during July 1st – July 4th, 2018.

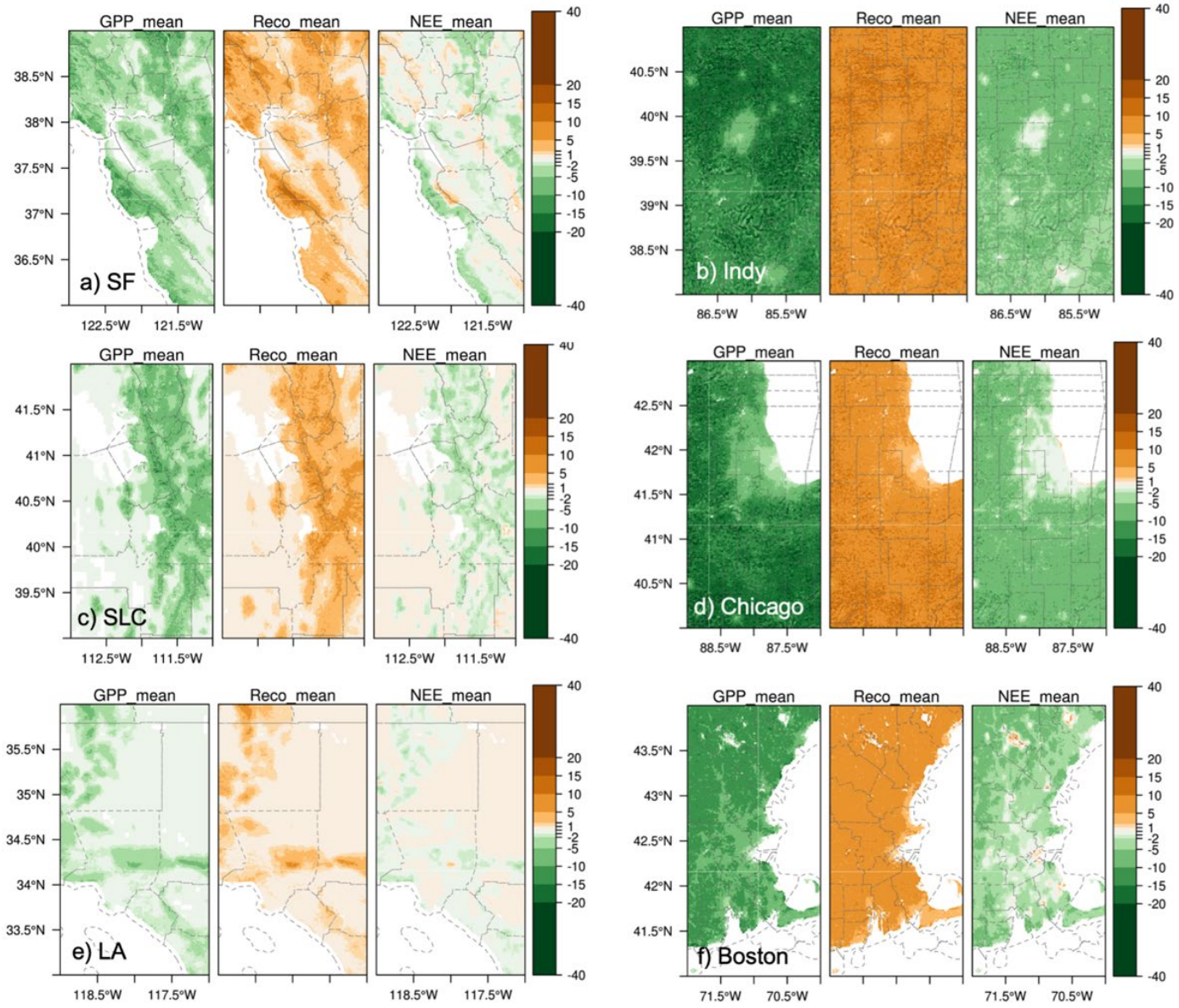

Figure S7. VCF-downscaled fluxes at 1km grid spacing [µmol m-2 s-1] zoomed into selected western vs. eastern CONUS cities, averaged over JJA 2018. Colour scales are consistent among 6 urban areas.

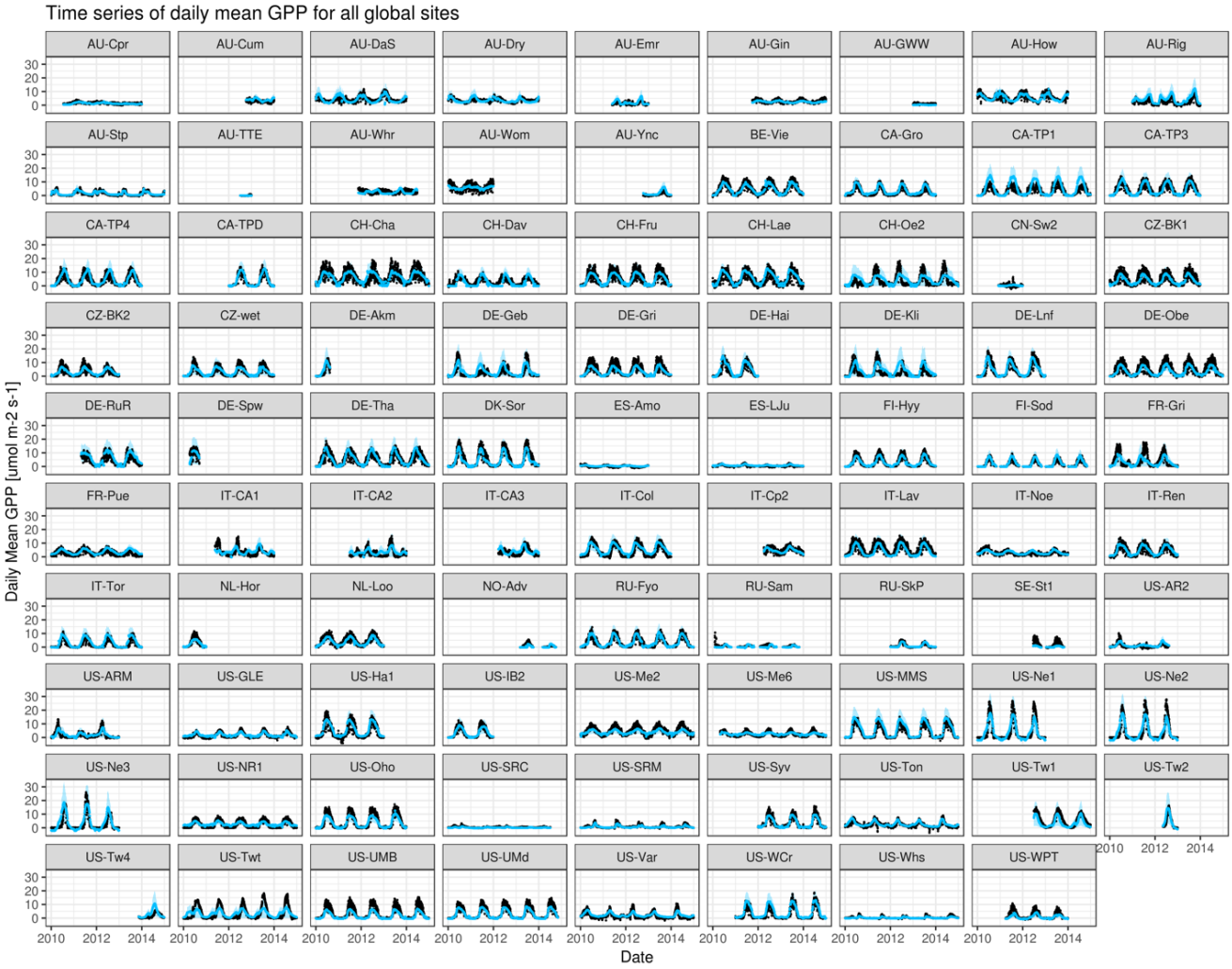

Figure S8. Time series of 4-day mean GPP between SMUrF (blue lines with uncertainties in blue ribbons) and FLUXNET (black dots) for 89 global EC sites from 2010 to 2014. Note that these modeled GPP are directly computed using biome-specific GPP-SIF slopes and SIF extracted at EC sites locations before aggregating to 0.050.05°. These modeled fluxes differ from the values extracted from the 0.05° gridded fields (e.g., hourly NEE shown in **Fig. S10**) that take the account of spatial variations in biome types in each 0.05° model grid.

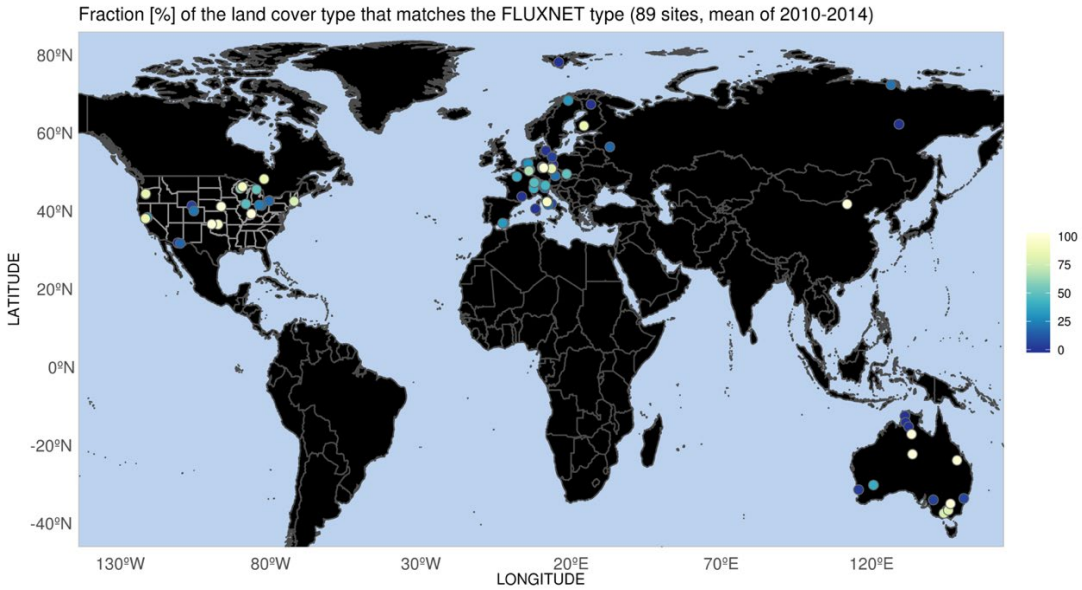

Figure S9. A simple measure of spatial heterogeneity in the 0.05° model grid cell, i.e., the percentage of the land cover types that matches those indicated by EC sites from FLUXNET2015 over all the land cover types at 500 m according to MCD12Q1.

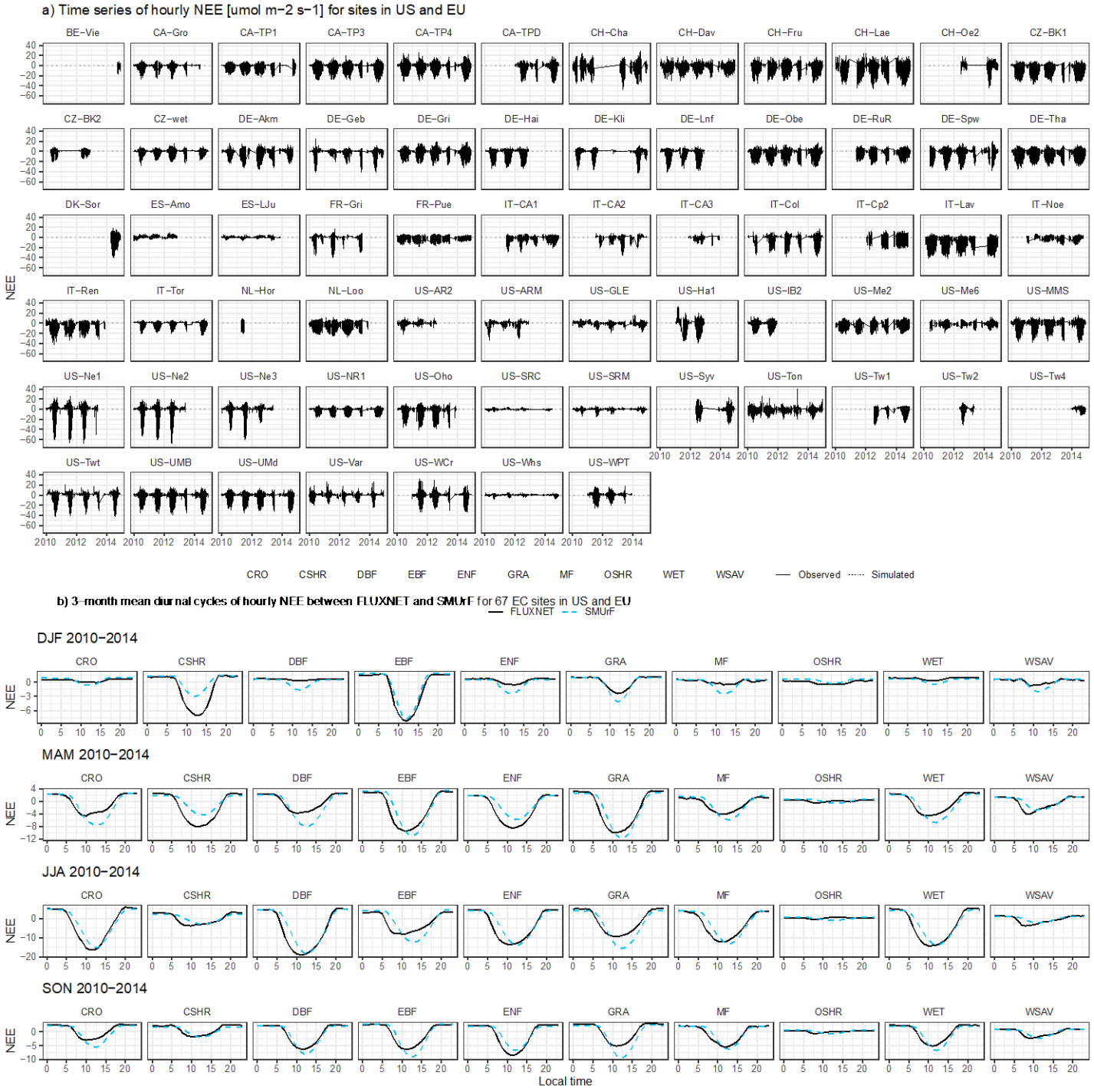

Figure S10. a) Time series of model-data comparisons of hourly NEE between modeled values extracted from the 0.05° SMUrF field (coloured dashed lines with colours differentiating biome types) and FLUXNET (black solid lines) during 2010-2014. Only non-gapfilled measured NEE data from 67 EC sites in US and Europe has been selected for the comparison. **b)** 3-month mean diurnal cycles of modeled (dashed blue lines) and measured NEE (black solid lines) per biome for the same sites.

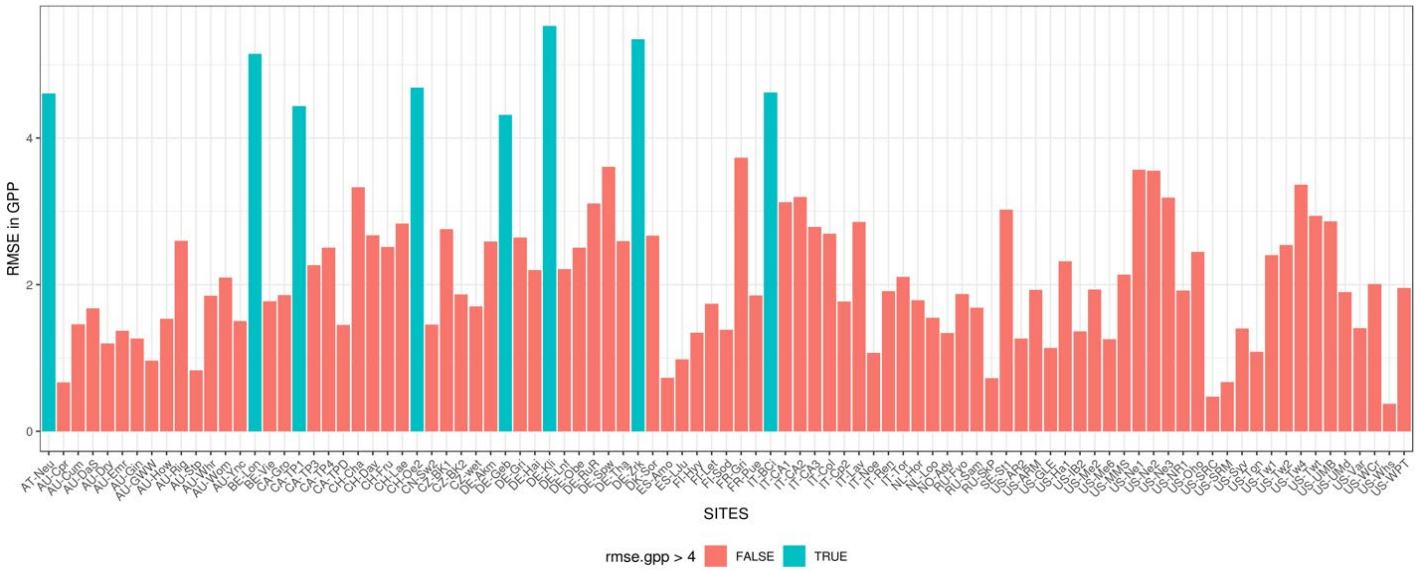

Figure S11. RMSE between modeled versus observed daily mean GPP for all 93 sites. Sites with relatively large GPP errors have been removed before training R_{eco}.

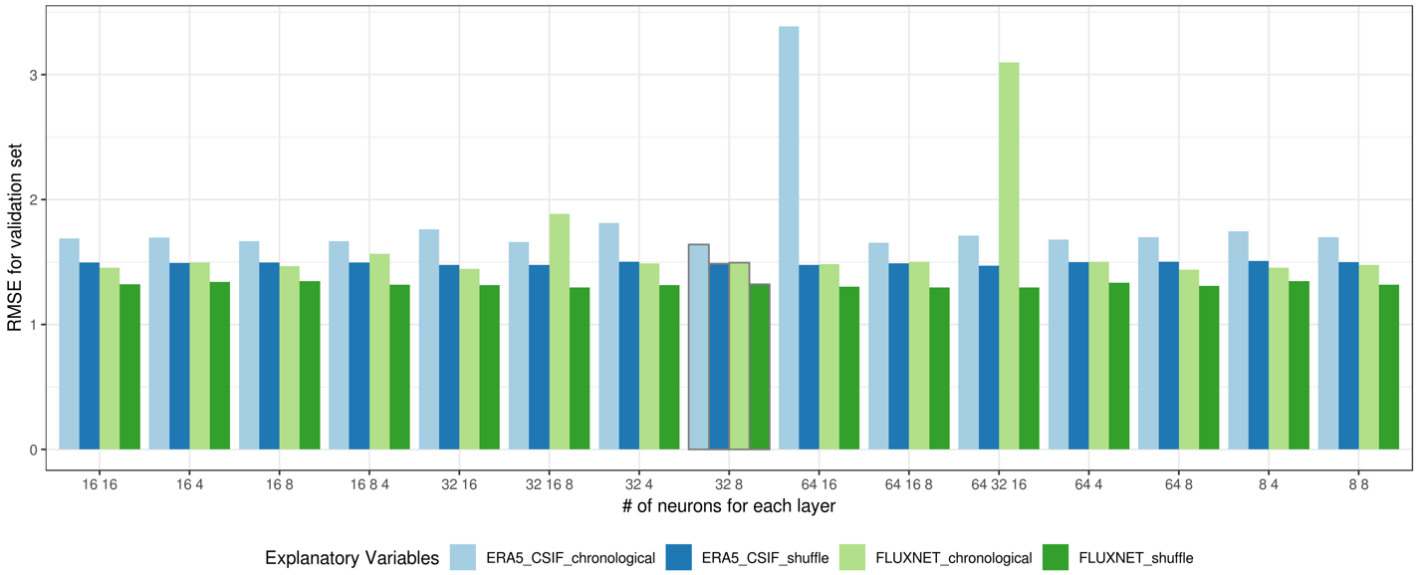

Figure S12. Overall RMSE between predicted and observed R_{eco} using different numbers of neurons per layers (labeled as x-axis) via a 5-fold cross validation following the M3 approach described in **Appendix B**. We tested four sets of neural network models using

1. ERA5-based temperatures and CSIF-based GPP **without** data shuffling before validation, i.e., data arranged in a chronological order from year 2010 to 2014 ('*ERA5_CSIF_chronological*');
2. ERA5-based temperatures and CSIF-based GPP **with** data shuffling before validation ('*ERA5_CSIF_shuffle'*);
3. FLUXNET2015-based temperatures and GPP **without** data shuffling ('*FLUXNET_chronological*'); and
4. FLUXNET-based temperatures and GPP **with** data shuffling ('*FLUXNET_shuffle*').

Because this is a 5-fold cross validation, 5 RMSE for 5 holdouts have been aggregated to an overall value as shown in one bar. If data had not been shuffled before training, it is arranged in a chronological order. We ended up using 32 neurons for the first hidden layer and 8 neurons for the second layer as outlined in gray.